Therefore the Co–O lengths in these cobalt alkoxides suggest that the Co–O distance in **3** is rather long. This lends further support to the view that the $[OBMes_2]^-$ ligand is a less effective π-donor than alkoxides. The preservation of the short B–O distance is also good evidence for the multiple nature of the B–O bond. This fact, in combination with the suggestion of reduction in π-donor character in the cobalt complex above, indicates that the $[OBMes_2]^-$ will prove a useful ligand in other systems. The syntheses of earlier transition-metal complexes where the changes in M–O distances should be more clear-cut are underway.

The UV/vis absorption spectrum of **3** in THF is fully consistent with the X-ray structural data. The ^4F ground state for a Co^{2+} ion in a tetrahedral field is split into three states, $^4A_2$, $^4T_2$, and $^4T_1$, so that two absorptions may be expected. The imposition of a lowered C_{2v} symmetry on the basic T_d configuration splits the two T states, giving the observed total of four absorptions.

Acknowledgment. We thank the National Science Foundation and the donors of the Petroleum Research Fund, administered by the American Chemical Society, for financial support.

Supplementary Material Available: Tables of bond distances and angles, anisotropic thermal parameters, and hydrogen coordinates (11 pages); tables of structure factors (49 pages). Ordering information is given on any current masthead page.

Contribution from the Department of Chemistry, University of California, Davis, California 95616

A Novel Case of Metal–Metal Bond Mobility. Structure and Fluxional Behavior of $[Rh_2Pd(CO)_2(\mu\text{-}Cl)Cl_2\{\mu\text{-}(Ph_2PCH_2)_2AsPh\}_2][BPh_4]$ and Related Compounds

D. Andan Bailey, Alan L. Balch,* L. Alan Fossett, Marilyn M. Olmstead, and Philip E. Reedy, Jr.

Received December 5, 1986

Treatment of the metallamacrocycle $Rh_2(CO)_2Cl_2(\mu\text{-dpma})_2$ (dpma is bis((diphenylphosphino)methyl)phenylarsine) with bis(benzonitrile)palladium(II) chloride results in the introduction of palladium into the center of the macrocycle to form $[Rh_2Pd(CO)_2(\mu\text{-Cl})Cl_2(\mu\text{-dpma})_2]^+$, which has been isolated as the tetraphenylborate salt. The corresponding bromide and iodide complexes have been prepared by metathesis. An analogous iridium complex, $[Ir_2Pd(CO)_2(\mu\text{-Cl})Cl_2(\mu\text{-dpma})_2]^+$, has been prepared. Red parallelepipeds of $[Rh_2Pd(CO)_2(\mu\text{-Cl})Cl_2(\mu\text{-dpma})_2][BPh_4]\cdot 2CH_2Cl_2\cdot(C_2H_5)_2O$ were grown by diffusion of ethyl ether into a dichloromethane solution of **5**. They belong to the monoclinic space group $P2_1/n$ (No. 14) with $a = 20.354$ (3) Å, $b = 14.494$ (3) Å, $c = 32.987$ (5) Å, and $\beta = 104.65$ (1)° at 140 K, $Z = 4$, and $R = 0.071$ for 11 021 reflections with $I > 2\sigma(I)$ and 535 parameters. The cation contains a palladium at the center of the original macrocycle. The palladium is bound to two trans arsines, a bridging chloride, and Rh(2). A Pd–Cl bond has oxidatively added to Rh(2), which has as ligands two trans phosphines, two chloride ligands, a terminal carbon monoxide, and the palladium ion (Pd–Rh(2), 2.699 (1) Å). Rh(1) has as ligands two trans phosphines, a terminal carbonyl, and a bridging chloride. ^{31}P and ^{13}C NMR data in solution indicate that a fluxional process renders the two ends of $[Rh_2Pd(CO)_2(\mu\text{-Cl})Cl_2(\mu\text{-dpma})_2]^+$ equivalent through a process that must relocate the chloride ligands and the Rh–Pd bond. The mechanism of this process is discussed in the context of experimental observations.

Introduction

The metallamacrocycles $Rh_2(CO)_2Cl_2(\mu\text{-dpma})_2$ (**1**) and $Ir_2(CO)_2Cl_2(\mu\text{-dpma})_2$ (**2**) (dpma is bis((diphenylphosphino)methyl)phenylarsine) have central cavities that are capable of binding a variety of metal ions, as shown schematically in eq 1.[1,2]

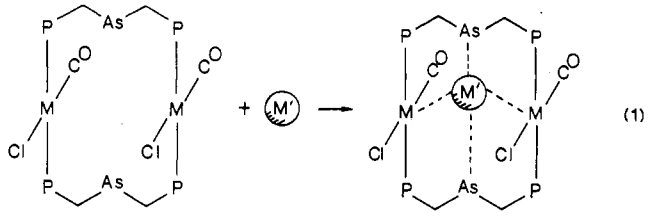

1, M = Rh
2, M = Ir

We have reported on the systematic synthesis of a series of complexes, **3** and **4**, with nearly linear Rh_3, RhIrRh, IrRhIr, and Ir_3

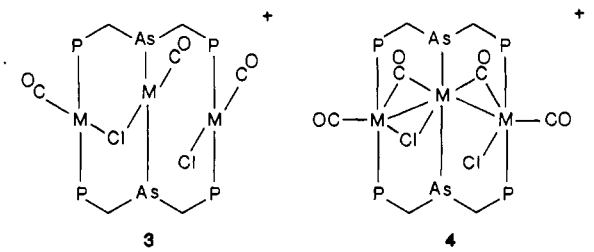

3 **4**

chains.[2] In solution these cations, and an analogous Rh_3 chain involving the corresponding triphosphine, bis((diphenylphosphino)methyl)phenylphosphine (=dpmp), undergo facile bridge/terminal halide exchange, which renders the two end metal environments equivalent.[3,4] The insertions of palladium(II) into **1** and **2** have also been briefly described.[1] Here we report details of this reaction, structural characterization of the products, and delineation of the fluxional behavior of these mixed-metal species.

Results

Synthetic Studies. Treatment of **1** with bis(benzonitrile)palladium(II) chloride in dichloromethane solution yields a deep red solution from which red crystals of $[Rh_2Pd(CO)_2(\mu\text{-Cl})Cl_2(\mu\text{-dpma})_2][BPh_4]$ (**5**) are obtained in 75% yield upon precipitation

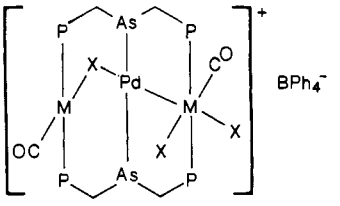

5, M = Rh, X = Cl
6, M = Rh, X = Br
7, M = Rh, X = I
8, M = Ir, X = I
9, M = Ir, X = Cl

with a methanol solution of sodium tetraphenylborate. Because a change in the halide ligand produces significant structural changes in complexes of the $[M_3(\mu\text{-dpmp})_2(CO)_3X_2]^+$ or $[M_3(\mu\text{-dpma})_2(CO)_3X_2]^+$ type,[3] the effect of exchanging chloride for

(1) Balch, A. L.; Fossett, L. A.; Olmstead, M. M.; Oram, D. E.; Reedy, P. E., Jr. *J. Am. Chem. Soc.* **1985**, *107*, 5272.
(2) Balch, A. L.; Fossett, L. A.; Olmstead, M. M.; Reedy, P. E., Jr. *Organometallics* **1986**, *5*, 1929.
(3) Balch, A. L.; Fossett, L. A.; Guimerans, R. R.; Olmstead, M. M.; Reedy, P. E., Jr.; Wood, F. E. *Inorg. Chem.* **1986**, *25*, 1248.
(4) Balch, A. L.; Fossett, L. A.; Guimerans, R. R.; Olmstead, M. M.; Reedy, P. E., Jr. *Inorg. Chem.* **1986**, *25*, 1397.

0020-1669/87/1326-2413$01.50/0

Table I. Infrared and UV–Visible Spectral Data

compd	IR ν(CO), cm^{-1} [a]	UV–vis λ, nm (ϵ, cm^{-1} M^{-1})
$Rh_2(CO)_2Cl_2(\mu\text{-dpma})_2$ (**1**)	1985, 1974	367 (9570)
$Ir_2(CO)_2Cl_2(\mu\text{-dpma})_2$ (**2**)	1974, 1964	432 (1900)
		383 (1600)
		335 (7600)
$[Rh_2Pd(CO)_2(\mu\text{-Cl})Cl_2(\mu\text{-dpma})_2][BPh_4]$ (**5**)	1987[b] (30)[c]	518 (5500)
		354 (22 100)
$[Rh_2Pd(CO)_2(\mu\text{-Br})Br_2(\mu\text{-dpma})_2]$-$[BPh_4]$ (**6**)	1976 (10)[c]	548 (7100)
		377 (19 600)
		320 (22 000)
$[Rh_2Pd(CO)_2(\mu\text{-I})I_2(\mu\text{-dpma})_2][BPh_4]$ (**7**)	1970 (22)[c]	584 (7000)
		386 (21 900)
$[Ir_2Pd(CO)_2(\mu\text{-I})I_2(\mu\text{-dpma})_2][BPh_4]$ (**8**)	1985, 1958	530 (10 000)
		418 (11 100)
		352 (18 500)
		310 (20 400)
$[Ir_2Pd(CO)_2(\mu\text{-Cl})Cl_2(\mu\text{-dpma})_2][BPh_4]$ (**9**)	2012, 1974	550 (7800)
		410 (9100)
		310 (16 000)

[a] Nujol mulls. [b] 1994 cm^{-1} in CH_2Cl_2 solution; width at half-height 20 cm^{-1}. [c] Width at half-height.

Table II. ^{31}P and ^{13}C NMR Spectral Data

	^{31}P NMR[a]		^{13}C NMR[a]		
compd	δ, ppm	^1J(Rh,P), Hz	δ, ppm	^1J(Rh,C), Hz	^2J(P,C), Hz
1	24.7	120	187.9	75.5	15
2	18.4		172.1		9.3
5	19.1	117[b]	186.2	67[c]	
	14.9	84	185.5	76	15
6	20.3	112[b]			
	12.4	85			
7	17.4	112[b]			
	3.7	86			
8	7.0				
	−36.5				
9	12.5		168.6		
	17.8		163.0		6.2

[a] Spectra taken at 25 °C unless otherwise noted. [b] Taken at −75 °C. [c] Taken at −25 °C.

bromide or iodide in **5** was investigated. Treatment of **5** with solutions of sodium bromide and sodium iodide in methanol at −25 °C results in clean exchange of the anions to yield **6** and **7**, respectively. Similarly, bis(benzonitrile)palladium(II) chloride reacts with **2**, sodium tetraphenylborate, and sodium iodide to give the iridium complex **8** as purple crystals in 80% yield with the chloro complex **9** as an intermediate.

Spectroscopic data for these complexes are collected in Tables I and II. These data indicate that all four have similar structures. All show only terminal carbonyl bands in the infrared spectra. For **5–7**, only a single ν(CO) is resolved. From the solid-state structure, it would appear that two absorptions are expected, since the environments of the two Rh–C–O groups differ. Two ^{13}C NMR resonances are observed for **5**. However, we have noted in other complexes that tilting of such a Rh–C–O group toward a metal–metal bond (vide infra) can result in significant lowering of ν(CO).[5] For example, in $Rh(CO)Cl_2(\mu\text{-}Ph_2Ppy)_2PdCl$ (Ph_2Ppy is 2-(diphenylphosphino)pyridine), which shows no tilting, ν(CO) is 2053 cm^{-1},[6] whereas in $Rh(CO)Cl_2(\mu\text{-dapm})_2PtCl$ (dapm is (diphenylphosphino)(diphenylarsino)methane) and $Rh(CO)I_2(\mu\text{-dapm})_2PtI$, which show appreciable tilting, ν(CO) is 2006 and 1985 cm^{-1}, respectively.[5] For **8** and **9**, two carbon monoxide stretching vibrations are resolved. The cause of this difference is not readily apparent; perhaps an Ir–C–O unit is less prone to such tilting.

Table III. Atomic Coordinates ($\times 10^4$) and Thermal Parameters ($Å^2 \times 10^3$) for $[Rh_2Pd(CO)_2(\mu\text{-Cl})Cl_2(\mu\text{-dpma})_2][BPh_4]\cdot 2CH_2Cl_2\cdot(C_2H_5)_2O$[a]

atom	x	y	z	U
Pd	6017 (1)	3803 (1)	3944 (1)	15 (1)[b]
Rh(1)	6613 (1)	1784 (1)	4125 (1)	17 (1)[b]
Rh(2)	6478 (1)	5150 (1)	3523 (1)	15 (1)[b]
As(1)	6776 (1)	4288 (1)	4581 (1)	16 (1)[b]
As(2)	5233 (1)	3259 (1)	3325 (1)	15 (1)[b]
P(1)	7372 (2)	2271 (2)	4736 (1)	20 (1)[b]
P(2)	7353 (2)	5715 (2)	4092 (1)	17 (1)[b]
P(3)	5935 (2)	1299 (2)	3489 (1)	17 (1)[b]
P(4)	5829 (2)	4704 (2)	2849 (1)	18 (1)[b]
Cl(1)	6800 (2)	6441 (2)	3135 (1)	23 (1)[b]
Cl(2)	5678 (2)	2515 (2)	4323 (1)	19 (1)[b]
Cl(3)	7305 (2)	4049 (2)	3435 (1)	25 (1)[b]
Cl(4)	2531 (2)	7065 (3)	1441 (1)	52 (2)[b]
Cl(5)	1225 (2)	6330 (3)	980 (1)	54 (2)[b]
Cl(6)	6087 (4)	3699 (5)	346 (2)	17 (2)
Cl(7)	5470 (4)	5342 (6)	579 (3)	34 (2)
O(1)	7663 (5)	470 (7)	4032 (3)	49 (3)
O(2)	5329 (4)	6010 (6)	3794 (3)	29 (2)
O(3)	5455 (6)	7583 (8)	1740 (4)	81 (4)
C(1)	7264 (7)	1011 (9)	4056 (4)	33 (4)
C(2)	5766 (6)	5673 (8)	3686 (4)	25 (3)
C(3)	7516 (6)	1372 (8)	5131 (4)	20 (3)
C(15)	7126 (6)	3307 (7)	4980 (4)	19 (3)
C(22)	7594 (5)	4832 (7)	4508 (3)	15 (3)
C(47)	5125 (5)	1924 (7)	3326 (4)	18 (3)
C(54)	5569 (6)	3506 (7)	2837 (3)	17 (3)

[a] Coordinates of the 84 phenyl ring carbons and boron are available as supplementary material. [b] Equivalent isotropic U defined as one-third of the trace of the orthogonalized U_{ij} tensor.

The low-temperature limiting ^{31}P NMR spectra of the complexes show two resonances. For the rhodium complexes, coupling to ^{103}Rh (spin 1/2; natural abundance 100%) is clearly resolved. For **5–7**, the high-field resonances exhibit the smaller P–Rh coupling constant as expected for an oxidized rhodium.[7] Consequently, these high-field resonances can be assigned to the six-coordinate rhodium centers that have undergone oxidation. The magnitudes of ^1J(P,Rh) for the low-field resonances are consistent with the presence of unaltered Rh(I) centers.[7] The ^{13}C NMR spectrum of **5** at −25 °C shows two equally intense resonances with couplings to ^{103}Rh or ^{31}P that are entirely appropriate for these structures.

X-ray Crystal Structure of $[Rh_2Pd(CO)_2(\mu\text{-Cl})Cl_2(\mu\text{-dpma})_2][BPh_4]\cdot 2CH_2Cl_2\cdot(C_2H_5)_2O$. The solid contains one cation, one entirely normal tetraphenylborate, two dichloromethane molecules, and an ethyl ether molecule in the asymmetric unit. There are no unusual contacts between these components. A perspective view of the cation with the atomic numbering scheme is shown in Figure 1. Atomic positional parameters are given in Table III. Tables IV and V give selected interatomic distances and angles, respectively. Although the cation has no crystallographically imposed symmetry, it has approximate C_s symmetry with the nearly planar $Rh_2Pd(CO)_2Cl_3$ portion, which is shown in a planar projection in Figure 2, acting as the mirror plane.

The structure of the cation shows that the basic framework of **1** has remained intact after complexation of the palladium ion. The palladium ion, however, is not symmetrically situated within the macrocycle. The Pd–Rh(2) distance (2.699 (1) Å) is consistent with a single bond between these two atoms. For comparison, the Pd–Rh distance in $RhPd(\mu\text{-}Ph_2Ppy)_2(CO)Cl_3$ is 2.594 (1) Å.[6] The other Pd···Rh distance is much longer, 3.166 (1) Å, and not consistent with a single bond between these atoms. The two rhodium centers are no longer equivalent in the cation. One, Rh(1), retains a nearly planar P_2CCl coordination sphere with its chloride ligand forming a fairly normal bridge to the palladium atom. The OC–Rh–Cl unit, however, is somewhat bent (C–Rh–Cl = 165.8 (5)°). The other rhodium, Rh(2), has undergone oxi-

(5) Balch, A. L.; Guimerans, R. R.; Linehan, J.; Olmstead, M. M.; Oram, D. E. *Organometallics* **1985**, *4*, 1445.
(6) Farr, J. P.; Olmstead, M. M.; Balch, A. L. *Inorg. Chem.* **1983**, *22*, 1229.
(7) Pregosin, P. S.; Kunz, R. W. *^{31}P and ^{13}C NMR Spectra of Transition Metal Complexes*; Springer Verlag: New York, 1979.

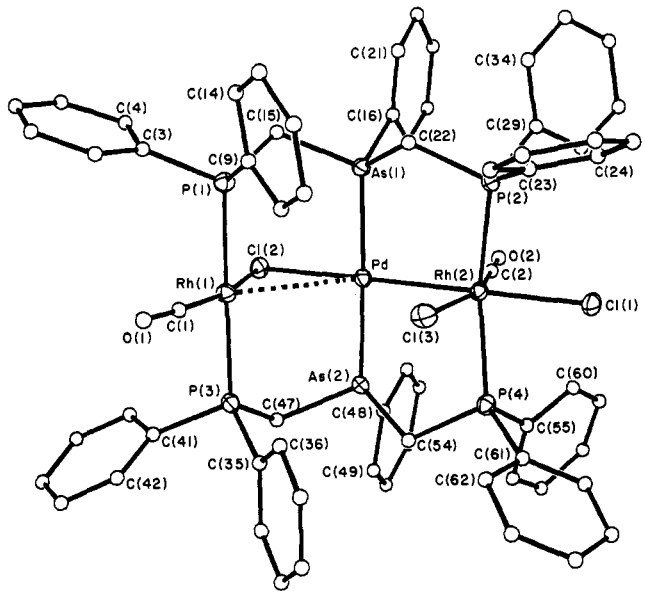

Figure 1. Perspective view of $[Rh_2Pd(CO)_2(\mu\text{-}Cl)Cl_2(\mu\text{-}dpma)_2]^+$, showing 50% thermal ellipsoids.

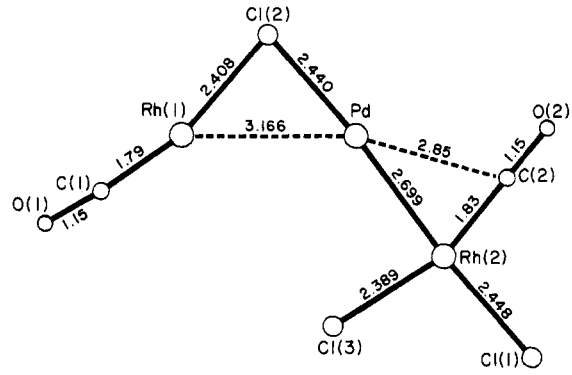

Figure 2. Planar section of $[Rh_2Pd(CO)_2(\mu\text{-}Cl)Cl_2(\mu\text{-}dpma)_2]^+$.

Table IV. Selected Interatomic Distances (Å) in $[Rh_2Pd(CO)_2(\mu\text{-}Cl)Cl_2(\mu\text{-}dpma)_2]^+$

		At Rh(1)	
Rh(1)–P(1)	2.317 (3)	Rh(1)–P(3)	2.310 (3)
Rh(1)–C(1)	1.792 (14)	Rh(1)–Cl(2)	2.408 (3)
Rh(1)···Pd	3.166 (1)	C(1)–O(1)	1.147 (17)
		At Rh(2)	
Rh(2)–P(2)	2.383 (3)	Rh(2)–P(4)	2.370 (3)
Rh(2)–Cl(1)	2.448 (3)	Rh(2)–Cl(3)	2.389 (3)
Rh(2)–C(2)	1.832 (14)	Rh(2)–Pd	2.699 (1)
C(2)–O(2)	1.148 (16)		
		At Pd	
Pd–As(1)	2.379 (1)	Pd–As(2)	2.384 (1)
Pd–Cl(2)	2.440 (3)	Pd–Rh(2)	2.699 (1)
Pd···Rh(1)	3.199 (1)		

dative addition of a Pd–Cl bond. Hence, it is six-coordinate with two trans phosphine ligands, two chloride ligands, one terminal carbon monoxide ligand, and the palladium. The Rh(2)–Cl(1) bond is significantly longer than the Rh(2)–Cl(3) bond. This is a result of the high structural trans effect of the Pd–Rh bond, which serves to lengthen the Rh(2)–Cl(1) bond. Similar effects have been seen in other, related metal–metal-bonded complexes.[8] The two dpma ligands are trans to one another in a partially bent form, which has been encountered in other related complexes[9] where these ligands span two metal–metal separations of considerably different distances, as is the case here. As a consequence of these two different Rh–Pd separations, the P–C–As angles at C(15) and C(47), which span the larger Rh(1)···Pd separation, are opened wider than the corresponding P–C–As angles at C(22) and C(54). Likewise, the nonbonded P(1)···As(1) and P(3)···As(2) separations are larger than the P(2)···As(1) and P(4)···As(2) separations but smaller than the Rh(1)···Pd separation that they bridge. Because of the constraint of the Pd–Rh(2) bond, the P(2)–Rh(2)–P(4) angle is pinched inward and the Pd–Rh(2) distance is less than nonbonded As(1)···P(2) and As(2)···P(4) separations.

The carbon monoxide ligand is tilted slightly toward the Pd–Rh bond. The Pd–Rh(2)–C(2) angle of 75.2 (4)° deviates significantly from the ideal of 90°. This is the largest such deviation within the complex. There is no unusual external contact that would appear to force this distortion. Consequently, we attribute this angular compression to a weak π-donor interaction between the carbon monoxide ligand and the 16-electron palladium ion. Very similar structural features have been seen previously in $Rh(CO)Cl_2(\mu\text{-}dapm)_2PtCl$ and $Rh(CO)I_2(\mu\text{-}dapm)_2PtI$. For $Rh(CO)_2Cl(\mu\text{-}dapm)_2PtCl$ the Rh–Pt distance is 2.692 (1) Å, the Pt···C distance is 2.94 (1) Å, and the Pt–Rh–C angle is 78.2 (3)°.[5]

Table V. Selected Interatomic Angles (deg) in $[Rh_2Pd(CO)_2(\mu\text{-}Cl)Cl_2(\mu\text{-}dpma)_2]^+$

		At Rh(1)	
P(1)–Rh(1)–P(3)	175.0 (1)	Cl(2)–Rh(1)–C(1)	165.8 (5)
P(1)–Rh(1)–Cl(2)	91.6 (1)	P(3)–Rh(1)–Cl(2)	92.8 (1)
P(1)–Rh(1)–C(1)	87.1 (4)	P(3)–Rh(1)–C(1)	89.2 (4)
		At Rh(2)	
P(2)–Rh(2)–P(4)	163.9 (1)	Pd–Rh(2)–Cl(1)	175.0 (1)
Cl(3)–Rh(2)–C(2)	161.0 (4)		
P(4)–Rh(2)–Pd	95.9 (1)	P(2)–Rh(2)–Pd	97.5 (1)
P(4)–Rh(2)–Cl(1)	83.0 (1)	P(2)–Rh(2)–Cl(1)	84.4 (1)
P(4)–Rh(2)–Cl(3)	87.0 (1)	P(2)–Rh(2)–Cl(3)	85.2 (1)
P(4)–Rh(2)–C(2)	95.4 (4)	P(2)–Rh(2)–C(2)	96.6 (4)
Pd–Rh(2)–Cl(3)	85.8 (1)	Cl(1)–Rh(2)–Cl(3)	99.0 (1)
Pd–Rh(2)–C(2)	75.2 (4)	Cl(1)–Rh(2)–C(2)	100.0 (4)
		At Pd	
As(1)–Pd–As(2)	177.1 (1)	Rh(2)–Pd–Cl(2)	175.5 (1)
As(1)–Pd–Cl(2)	88.8 (1)	As(2)–Pd–Cl(2)	88.4 (1)
As(1)–Pd–Rh(2)	90.5 (1)	As(2)–Pd–Rh(2)	92.4 (1)
		At Carbon Monoxide	
Rh(1)–C(1)–O(1)	174.7 (13)	Rh(2)–C(2)–O(1)	178.6 (11)
		At Bridging Chloride	
Rh(1)–Cl(2)–Pd	81.5 (1)		
		At Methylene Carbon	
P(1)–C(15)–As(1)	113.4 (6)	As(1)–C(22)–P(2)	107.6 (5)
P(3)–C(47)–As(2)	113.3 (5)	As(2)–C(54)–P(4)	108.8 (6)

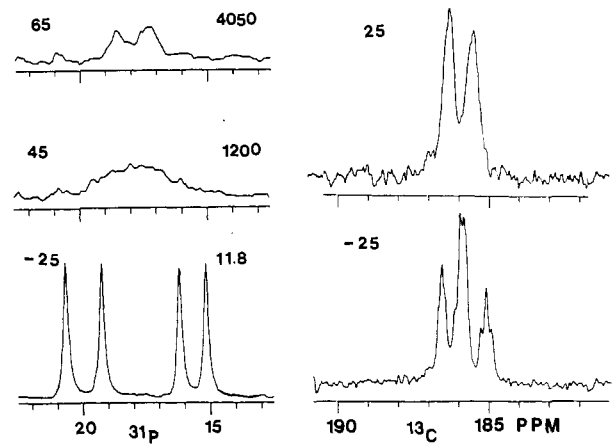

Figure 3. Left: 81-MHz $^{31}P\{^1H\}$ NMR spectra of $[Rh_2Pd(CO)_2(\mu\text{-}Cl)Cl_2(\mu\text{-}dpma)_2]^+$. Temperature (°C) is given to the left of each trace, while the rate constant ($\times 10^{-3}$ s^{-1}) derived by line shape analysis is given to the right. Right: $^{13}C\{^1H\}$ NMR spectra of $[Rh_2Pd(CO)_2(\mu\text{-}Cl)Cl_2(\mu\text{-}dpma)_2]^+$.

(8) Maisonnat, A.; Farr, J. P.; Olmstead, M. M.; Hunt, C. T.; Balch, A. L. *Inorg. Chem.* **1982**, *21*, 3961.
(9) Balch, A. L.; Fossett, L. A.; Guimerans, R. R.; Olmstead, M. M. *Organometallics* **1985**, *4*, 781.

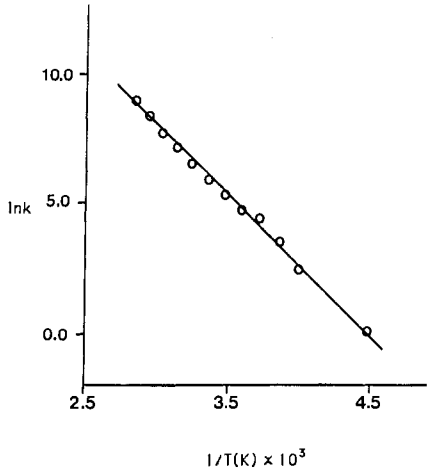

Figure 4. Plot of ln k vs. $1/T$ for $[Rh_2Pd(CO)_2(\mu\text{-}Cl)Cl_2(\mu\text{-}dpma)_2]^+$.

As we pointed out earlier, this tilting is responsible for lowering ν(CO) in the infrared spectrum of this cation.

Fluxional Behavior. The NMR spectra of **5** indicate that it is fluxional. The temperature-dependent ^{31}P NMR spectra in acetonitrile solution are shown on the left side of Figure 3. At low temperature, two equally intense doublets are observed; each represents a unique phosphorus environment with coupling to the coordinated rhodium. This spectrum is that expected from the solid-state crystallographic data. On warming, the resonances broaden, merge, and reappear at 65 °C as a broad doublet. The doublet splitting of 101 Hz is the average of the two low-temperature ^1J(P,Rh) values. Thus, the phosphines remain coordinated to the rhodium atoms during a process that renders the two RhP_2 units equivalent. Warming above 65 °C results in decomposition of the complex, but below that, the temperature-dependent changes of Figure 3 are reversible. Changing the concentration of **5** has no effect on the line widths at fixed temperatures; hence, the process is intraionic. The spectra have been satisfactorily simulated and analyzed to give rate constants (k) for the two-site exchange. These are shown on the right of each spectral trace in Figure 3, and more extensive data are given in supplementary material. An Arrhenius plot of the data is shown in Figure 4. From this, E_a is 10.5 (0.7) kcal/mol, and from an Eyring plot, $\Delta H^\ddagger$ = 9.9 (0.7) kcal/mol, $\Delta S^\ddagger$ = −13.1 (0.9) eu, and $\Delta G^\ddagger$ = 13.8 (0.2) kcal/mol.

The ^{13}C NMR spectra of ^{13}CO-enriched **5** are also indicative of this process. At −25 °C the complex pattern seen on the right of Figure 3 can be analyzed in terms of two doublets arising from two distinct ^{13}C atoms, each of which is coupled to a directly bound rhodium. Further splitting of the upfield doublet is due to ^2J(P,C), which creates an additional triplet pattern. The upfield half of the doublet at 186.2 ppm and the downfield half of the doublet at 185.5 ppm overlap. On warming to 25 °C, only a single doublet at 185.9 ppm is seen in Figure 3 as a result of a dynamic process that renders the two carbon monoxide ligands equivalent while retaining the Rh–CO bonding.

These results indicate that a dynamic process occurs that makes the two end groups in **5** equivalent. As a result, the palladium atom must move back and forth, making and breaking the Rh–Pd bond as well as the Pd–Cl(bridge) bond. The other ligands must move as well. Since one rhodium atom is bound to two chloride ligands and the other to only one, the fluxional path must account for migration of a chloride ligand. The simplest process would involve chloride dissociation and migration to the opposite end as shown in Scheme I. This process can effectively be ruled out by experimental observations. Addition of chloride ion to the system produces no change in line shape (i.e. rate) at the temperatures involved. Likewise, addition of the chloride scavenger, $[Ir_2Rh(CO)_5Cl(\mu\text{-}dpma)_2]^{2+}$ [10] (which reacts with chloride, as the tetraphenylarsonium salt, in dichloromethane to form $[Ir_2Rh(\mu\text{-}CO)_2(CO)_2(\mu\text{-}Cl)Cl(\mu\text{-}dpma)_2]^+$),[10] has no effect on line shapes. Finally, $\Delta S^\ddagger$ for the process is negative, whereas a dissociative step would be expected to be accompanied by a positive $\Delta S^\ddagger$.

Scheme I

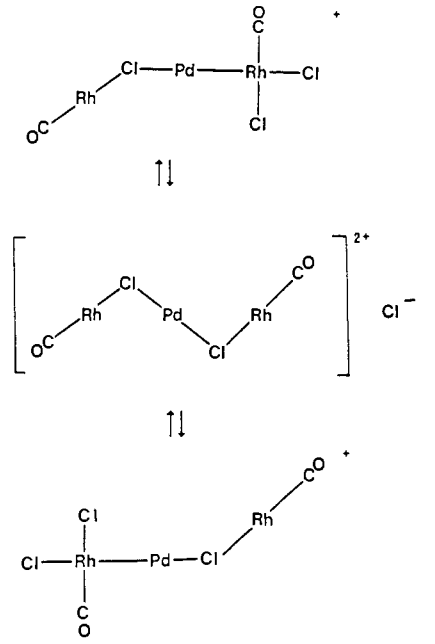

Scheme II presents an alternative process in which all ligands remain bound during its operation. Only the ligands in the plane displayed in Figure 2 are shown; the bridging dpma ligands lie above and below this plane. Here fluxionality results from a series of terminal/bridge interchanges of halide ligands as well as opening and closing of the Pd–Rh bonds. Similar, but simpler, bridge/terminal interchanges have been proposed for complexes **3** and **4**.

Similar dynamic behavior has been observed in the ^{31}P NMR spectrum of the bromo complex **6**. Line shape analysis of the variable-temperature spectra in acetonitrile solution yields E_a = 12.6 (1.0) kcal/mol from the Arrhenius plot, while the Eyring plot gives $\Delta G^\ddagger$ = 14.0 (0.2) kcal/mol, $\Delta H^\ddagger$ = 12.0 (1.0) kcal/mol, and $\Delta S^\ddagger$ = −6.8 (0.5) eu. The negative values of $\Delta S^\ddagger$ observed for **5** and **6** are inconsistent with a process that involves any ligand dissociation (particularly chloride dissociation) from these cations during the fluxional process. Thus these measurements also favor the process shown in Scheme II over that shown in Scheme I.

The iodide complex **7** also shows similar behavior, but its low solubility limited our measurements to evaluating $\Delta G^\ddagger$ = 14.3 (0.2) kcal/mol. Likewise, the ^{31}P NMR spectrum of the iridium complex **8** shows line broadening upon warming. Although coalescence was not achieved, we can calculate that $\Delta G^\ddagger$ = 16.2 (0.2) kcal/mol. The higher barrier for this iridium compound **8** in comparison to its rhodium analogue **7** is consistent with the greater metal–ligand bond strength of the heavier metal.

Experimental Section

Preparation of Compounds. The ligand dpma[1] and complexes **1**[1] and **2**,[1] as well as bis(benzonitrile)palladium(II) chloride,[11] were prepared as described previously. Deoxygenated solvents and inert-atmosphere conditions were used in the synthesis of **5** and **8**, while no such precautions were required with **6** and **7**. The pure complexes are air stable both as solids and in solution.

$[Rh_2Pd(CO)_2(\mu\text{-}Cl)Cl_2(\mu\text{-}dpma)_2][BPh_4]$ (5). A solution of 26.8 mg (0.070 mmol) of $PdCl_2(NCPh)_2$ dissolved in 3 mL of dichloromethane was added slowly (15 min) with stirring to a cold (−20 °C) solution of 100 mg (0.070 mmol) of $Rh_2(CO)_2Cl_2(\mu\text{-}dpma)_2$ in 3 mL of dichloromethane. The reaction mixture turned dark red immediately. After the addition was complete, a solution of 60 mg (0.18 mmol) of sodium tetraphenylborate in 3 mL of methanol was added, whereupon the red, crystalline product precipitated. An additional 4 mL of methanol was

(10) Balch, A. L.; Fossett, L. A.; Olmstead, M. M.; Reedy, P. E., Jr., to be submitted for publication.

(11) Holden, J. R.; Baenziger, N. C. *Acta Crystallogr.* **1956**, *9*, 194.

Scheme II

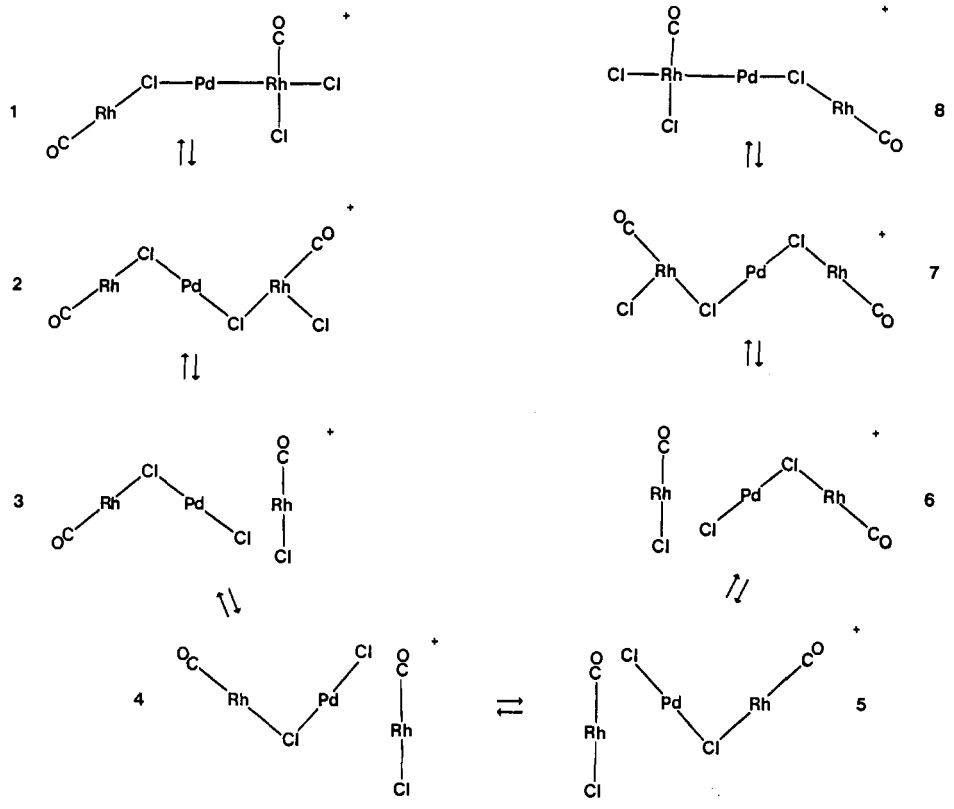

added to ensure complete precipitation of the product. The product was collected by filtration and washed successively with methanol and diethyl ether. It was purified by dissolving it in a minimum amount of dichloromethane, filtering, and slowly adding diethyl ether; yield 80 mg, 63%.

$[Rh_2Pd(CO)_2(\mu\text{-Br})Br_2(\mu\text{-dpma})_2][BPh_4]$ (6). A solution of 70 mg (0.47 mmol) of sodium bromide in 2 mL of methanol was added with stirring to a cold (−20 °C) solution of 60 mg (0.032 mmol) of **5** in 2 mL of dichloromethane. The solution became violet. After several minutes of stirring, a solution of 200 mg (0.60 mmol) of sodium tetraphenylborate in 1 mL of methanol was added, causing violet crystals to precipitate. The product was collected by filtration and washed with methanol and diethyl ether; yield 60 mg, 93%. Anal. Calcd for $C_{90}H_{78}As_2BBr_3O_2P_4PdRh_2$: C, 53.72; H, 3.91; Br, 11.91. Found: C, 53.97; H, 4.07; Br, 11.96.

$[Rh_2Pd(CO)_2(\mu\text{-I})I_2(\mu\text{-dpma})_2][BPh_4]$ (7). A solution of 70 mg (0.47 mmol) of sodium iodide in 1 mL of methanol was added with stirring to a cold (−20 °C) solution of 60 mg (0.032 mmol) of **5** in 2 mL of dichloromethane. The solution immediately turned dark green. After several minutes of stirring, a solution of 200 mg (0.6 mmol) of sodium tetraphenylborate in 1 mL of methanol was added and green crystals precipitated. The product was collected by filtration and washed successively with methanol and diethyl ether; yield 64 mg, 92%. Anal. Calcd for $C_{90}H_{78}As_2BI_3O_2P_4PdRh_2$: C, 50.20; H, 3.65; I, 17.82. Found: C, 49.48; H, 3.53; I, 17.76.

$[Ir_2Pd(CO)_2(\mu\text{-I})I_2(\mu\text{-dpma})_2][BPh_4]$ (8). A solution of 23.8 mg (0.062 mmol) of $PdCl_2(NCPh)_2$ in 3 mL of dichloromethane was added slowly (15 min) with stirring to a cold (−20 °C) solution of 100 mg (0.062 mmol) of $Ir_2(CO)_2Cl_2(\mu\text{-dpma})_2$ in 3 mL of dichloromethane. The reaction mixture turned dark red immediately. After the addition was complete, a solution of 60 mg (0.18 mmol) of sodium tetraphenylborate in 3 mL of methanol was added to precipitate intermediate **9** as a red-brown powder. An additional 4 mL of methanol was added to ensure complete precipitation. Intermediate **9** was collected by filtration and washed with methanol and diethyl ether; yield 85 mg. The red-brown solid was then dissolved in 2 mL of dichloromethane and treated with sodium iodide and sodium tetraphenylborate by using the same procedure for the preparation of **7**. An additional 3 mL portion of methanol was added to ensure complete precipitation of the violet, crystalline product. The product was washed with methanol and diethyl ether; overall yield 80 mg, 65%. Anal. Calcd for $C_{90}H_{78}As_2BI_3Ir_2O_2P_4Pd$: C, 46.36; H, 3.37; I, 16.46. Found: C, 44.75; H, 3.17; I, 16.44.

Spectroscopic Measurements. The ^{31}P NMR spectra were recorded with proton decoupling on a Nicolet NT-200 Fourier transform spectrometer operating at 81 MHz. ^{13}C NMR spectra were recorded at 90.5 MHz on a Nicolet NT-360 FT spectrometer. References: ^{31}P, external

Table VI. Crystal Data and Data Collection Parameters for $[Rh_2Pd(CO)_2(\mu\text{-Cl})Cl_2(\mu\text{-dpma})_2][BPh_4]\cdot 2CH_2Cl_2\cdot(C_2H_5)_2O$

formula	$PdRh_2As_2Cl_7P_4O_3C_{96}BH_{92}$
fw	2138.8
cryst system	monoclinic
space group	$P2_1/n$
syst absences	$0k0$, $k = 2n$; $h0l$, $h + l = 2n$
cryst dimens, mm	0.175 × 0.20 × 0.32
cryst color and habit	red parallelepipeds
a, Å (140 K)	20.354 (3)
b, Å	14.494 (3)
c, Å	32.987 (5)
β	104.65 (1)
V, Å^3	9415 (3)
Z	4
$d(140\ K)_{calcd}$, g/cm^3	1.51
radiation; λ, Å (graphite monochrometer)	Mo Kα; 0.071 069
linear abs coeff, cm^{-1}	11.5
temp, K	140
instrument	Syntex $P2_1$, bisecting mode
scan speed, deg/min.	8
scan width, deg	1
type of scan	ω
ω offset for bkgds, deg	1
2θ range, deg	0–50
range of transmission factors	0.78–0.85
octants	$h,k,\pm l$
no. of variables	535
data/variable ratio	20.6
programs	SHELXTL, version 4
check reflcns	3 every 198 reflecns; 2.7% decay
no. of data collected	17 748
no. of unique data	16 530
R merge	0.025
no. of data ($I \geq 2\sigma(I)$) used in refinement	11 021
$R(F)$	0.071
$R_w(F)$	0.060
largest Δ/σ	0.067 (overall scale)

85% phosphoric acid; ^1H and ^{13}C, internal tetramethylsilane. The high-frequency-positive convention, recommended by IUPAC, has been used in reporting all chemical shifts. Line shape analyses of ^{31}P NMR spectra were performed with an iterative analysis program, DNMR5,[12,13] on a VAX/VMS computer. Infrared spectra (resolution 2 cm^{-1}) were recorded from mineral oil mulls or dichloromethane solutions with a Perkin-Elmer 180 spectrometer. Electronic spectra were recorded on a Hewlett-Packard 8450A.

X-ray Data Collection, Solution, and Refinement for $[Rh_2Pd(CO)_2(\mu\text{-}Cl)Cl_2(\mu\text{-dpma})_2][BPh_4]\cdot 2CH_2Cl_2\cdot(C_2H_5)_2O$. Well-formed red parallelepipeds were grown by slow diffusion of diethyl ether into a dichloromethane solution of the complex. The crystals were rapidly taken from the diffusion tube and covered with epoxy resin to reduce loss of solvent from the crystal. Crystal data, data collection procedures, and refinement of the structure are summarized in Table VI. The lattice was found to be monoclinic by standard procedures using the software associated with the Syntex $P2_1$ diffractometer. The data were corrected for Lorentz and polarization effects.

The structure was solved by locating the two rhodium and palladium atoms by using the Patterson method (FMAP 8 routine of SHELXTL, version 4, 1984, Nicolet Instrument Corp., Madison, WI). Other atoms were located from successive difference Fourier maps. Final cycles of refinement were made with anisotropic thermal parameters for iridium, rhodium, arsenic, phosphorus, and the five chlorine atoms, and isotropic thermal parameters for all remaining atoms. Hydrogen atoms were refined by using a riding model in which an idealized C-H vector of 0.96-Å length is recalculated with each cycle of refinement. Isotropic hydrogen thermal parameters were fixed at 1.2 times the equivalent isotropic thermal parameter of the bonded carbon. Scattering factors and corrections for anomalous dispersion were taken from a standard source.[14] An absorption correction (XABS) was applied.[15] One molecule of dichloromethane and the ether molecule exhibited large thermal motion. Ten reflections suffering from extinction were removed from the data set for the final cycles of refinement. A conventional R factor of 0.071 was obtained. The final difference map showed some residual electron density (3.7 e $Å^{-3}$), which may be part of a disordered dichloromethane since it is approximately 3 Å from a symmetry-related site. The next four are all in the vicinity of the less well-behaved of the two dichloromethane molecules.

Acknowledgment. We thank the National Science Foundation (Grant CHE8519557) for financial support and Dow Corning Corp. for a fellowship for P.E.R.

Registry No. **1**, 97551-38-7; **2**, 97570-01-9; **5**, 97551-42-3; **5**·$2CH_2Cl_2\cdot(C_2H_5)_2O$, 97551-43-4; **6**, 108818-13-9; **7**, 108818-15-1; **8**, 108818-17-3; **9**, 97551-40-1; $PdCl_2(NCPh)_2$, 14220-64-5; Pd, 7440-05-3; Rh, 7440-16-6.

Supplementary Material Available: Listings of anisotropic thermal parameters, hydrogen atom positions, phenyl carbon and boron positions, and bond distances and bond angles and a figure of extensive ^{31}P NMR data (12 pages); calculated and observed structure factor tables (65 pages). Ordering information is given on any current masthead page.

(12) Stephenson, D. S.; Binsch, G. *QCPE* **1978**, *No. 365*.
(13) Binsch, G. In *Dynamic Nuclear Magnetic Resonance Spectroscopy*; Jackson, L. M., Cotton, F. A., Eds.; Academic: New York, 1975; p 45.
(14) *International Tables for X-ray Crystallography*; Kynoch: Birmingham, England, 1974; Vol. 4.
(15) The method obtains an empirical absorption tensor from an expression relating F_o and F_c: Moezzi, B. Ph.D. Thesis, University of California, Davis, CA, 1986.

Contribution from the Departments of Chemistry, University of Glasgow, Glasgow G12 8QQ, Scotland, and The University of Western Ontario, London, Canada N6A 5B7

Synthesis and Structure of Pt_2Au Cluster Complexes, Including $[Pt_2(C{\equiv}C\text{-}t\text{-}Bu)_2(\mu\text{-}AuI)(\mu\text{-}Ph_2PCH_2PPh_2)_2]$

Ljubica Manojlović-Muir,*[1a] Kenneth W. Muir,[1a] Ilse Treurnicht,[1b] and Richard J. Puddephatt*[1b]

Received October 7, 1986

Reaction of $[Pt_2(\mu\text{-dppm})_3]$ (dppm = $Ph_2PCH_2PPh_2$) with AuCC-*t*-Bu gave the complex $[Pt_2(CC\text{-}t\text{-}Bu)_2(\mu\text{-AuX})(\mu\text{-dppm})_2]$ (**1a** (X = CC-*t*-Bu)), and this could be converted to the derivatives **1b** (X = Cl) and **1c** (X = I). The compounds are the first Pt_2Au clusters. The compound **1c**, fully characterized by X-ray diffraction, is a distorted molecular A-frame containing a 42-electron triangular Pt_2Au cluster with 3-center 2-electron metal-metal bonding [Pt-Au = 2.656 (2), 2.661 (2) Å and Pt-Pt = 2.837 (1) Å]. The crystals of **1c** are orthorhombic, space group $Pna2_1$ (No. 33), with $Z = 4$, $a = 29.053$ (4) Å, $b = 16.131$ (3) Å, and $c = 13.956$ (3) Å; $R = 0.040$ for 225 parameters refined from 4442 unique reflections with $I \geq 3\sigma(I)$.

Introduction

There has been much interest in the heteronuclear cluster complexes containing both a platinum-group metal and a coinage metal, and a number of synthetic routes to such compounds have been developed.[2-9] Most compounds containing Pt-Au bonds have been prepared by reactions of Ph_3PAu^+ with a platinum hydride[10] or an electron-rich cluster of platinum[11] and are based on the isolobal relationship for H^+ and Ph_3PAu^+.[12]

In this paper, the synthesis of the first Pt_2Au cluster complexes is reported, based on the reactions of AuCC-*t*-Bu. The latter

(1) (a) University of Glasgow. (b) The University of Western Ontario.
(2) Braunstein, P.; Rose, J. *Gold Bull.* **1985**, *18*, 17. Hall, K. P.; Mingos, D. M. P. *Prog. Inorg. Chem.* **1984**, *32*, 237.
(3) Schiaro, S. L.; Bruno, G.; Nicolò, F.; Piraino, P.; Faraone, F. *Organometallics* **1985**, *4*, 2091.
(4) Casalnuovo, A. L.; Laska, T.; Nilsson, P. V.; Olofson, J.; Pignolet, L. H. *Inorg. Chem.* **1985**, *24*, 182. Boyle, P. D.; Johnson, B. J.; Buehler, A.; Pignolet, L. H. *Inorg. Chem.* **1986**, *25*, 5.
(5) Ladd, J. A.; Hope, H.; Balch, A. L. *Organometallics* **1984**, *3*, 1838.
(6) Stone, F. G. A. *Angew. Chem., Int. Ed. Engl.* **1984**, *23*, 89.
(7) Uson, R. *Pure Appl. Chem.* **1986**, *58*, 647. Uson, R.; Forniés, J.; Tomas, M. *J. Am. Chem. Soc.* **1984**, *106*, 2482.
(8) Deeming, A. J.; Donovan-Mtunzi, S.; Hardcastle, K. *J. Chem. Soc., Dalton Trans.* **1986**, 543.
(9) Braunstein, P.; Rose, J.; Dedieu, A.; Dusausay, Y.; Mangeot, J.-P.; Tiripicchio, A.; Tiripicchio-Camellini, M. *J. Chem. Soc., Dalton Trans.* **1986**, 225.
(10) Braunstein, P.; Lehner, H.; Matt, D.; Tiripicchio, A.; Tiripicchio-Camellini, M. *Angew Chem., Int. Ed. Engl.* **1984**, *23*, 304.
(11) Briant, C. E.; Wardle, R. W. M.; Mingos, D. M. P. *J. Organomet. Chem.* **1984**, *267*, C49. Mingos, D. M. P. *J. Chem. Soc., Dalton Trans.* **1986**, 73. Briant, C. E.; Gilmour, D. I.; Mingos, D. M. P. *J. Chem. Soc., Dalton Trans.* **1986**, 835. Gilmour, D. I.; Mingos, D. M. P. *J. Organomet. Chem.* **1986**, *302*, 127.
(12) Lauher, J. W. *J. Am. Chem. Soc.* **1978**, *100*, 5305.

0020-1669/87/1326-2418$01.50/0